AMERICAN SOCIETY FOR MICROBIOLOGY | Antimicrobial Agents and Chemotherapy®

EXPERIMENTAL THERAPEUTICS

# Covalent Immobilization of Enoxacin onto Titanium Implant Surfaces for Inhibiting Multiple Bacterial Species Infection and *In Vivo* Methicillin-Resistant *Staphylococcus aureus* Infection Prophylaxis

**Bin'en Nie,[a] Teng Long,[a] Haiyong Ao,[a] Jianliang Zhou,[b] Tingting Tang,[a] Bing Yue[a,c]**

Shanghai Key Laboratory of Orthopedic Implants, Department of Orthopedic Surgery, Shanghai Ninth People's Hospital, Shanghai Jiao Tong University School of Medicine, Shanghai, People's Republic of China[a]; Department of Cardiothoracic Surgery, the Second Affiliated Hospital of Nanchang University, Nanchang, People's Republic of China[b]; Department of Joint Surgery and Sports Medicine, Shanghai Renji Hospital, Shanghai Jiao Tong University School of Medicine, Shanghai, People's Republic of China[c]

**ABSTRACT** Infection is one of the most important causes of titanium implant failure *in vivo*. A developing prophylactic method involves the immobilization of antibiotics, especially vancomycin, onto the surface of the titanium implant. However, these methods have a limited effect in curbing multiple bacterial infections due to antibiotic specificity. In the current study, enoxacin was covalently bound to an amine-functionalized Ti surface by use of a polyethylene glycol (PEG) spacer, and the bactericidal effectiveness was investigated *in vitro* and *in vivo*. The titanium surface was amine functionalized with 3-aminopropyltriethoxysilane (APTES), through which PEG spacer molecules were covalently immobilized onto the titanium, and then the enoxacin was covalently bound to the PEG, which was confirmed by X-ray photoelectron spectrometry (XPS). A spread plate assay, confocal laser scanning microscopy (CLSM), and scanning electron microscopy (SEM) were used to characterize the antimicrobial activity. For the *in vivo* study, Ti implants were inoculated with methicillin-resistant *Staphylococcus aureus* (MRSA) and implanted into the femoral medullary cavity of rats. The degree of infection was assessed by radiography, micro-computed tomography, and determination of the counts of adherent bacteria 3 weeks after surgery. Our data demonstrate that the enoxacin-modified PEGylated Ti surface effectively prevented bacterial colonization without compromising cell viability, adhesion, or proliferation *in vitro*. Furthermore, it prevented MRSA infection of the Ti implants *in vivo*. Taken together, our results demonstrate that the use of enoxacin-modified Ti is a potential approach to the alleviation of infections of Ti implants by multiple bacterial species.

**KEYWORDS** immobilization, titanium, enoxacin, polyethylene glycol, methicillin-resistant *Staphylococcus aureus*, prosthesis-related infection

Titanium (Ti) has been widely used for orthopedic and dental implants, due to its excellent mechanical, physical, and chemical properties (1). However, bacterial adhesion and biofilm formation on Ti surfaces remain the most common cause of failure of Ti implants (2). Ti can be functionalized with oxhydryl and amino group, which can in turn tether biomolecules, giving the surface multiple biofunctionalities. The modification of Ti surfaces with antibacterial agents and the immobilization of anti-

**Received** 16 August 2016 **Returned for modification** 1 September 2016 **Accepted** 25 October 2016

**Accepted manuscript posted online** 31 October 2016

**Citation** Nie B, Long T, Ao H, Zhou J, Tang T, Yue B. 2017. Covalent immobilization of enoxacin onto titanium implant surfaces for inhibiting multiple bacterial species infection and *in vivo* methicillin-resistant *Staphylococcus aureus* infection prophylaxis. Antimicrob Agents Chemother 61:e01766-16. https://doi.org/10.1128/AAC.01766-16.



Address correspondence to Bing Yue, advbmp2@163.com.

B.N. and T.L. contributed equally to this article.

bacterial agents onto surfaces, including antibiotics, antimicrobial peptides, silver, copper, and zinc, have proven to be effective approaches to obtaining antibacterial Ti surfaces (2–6). Of these agents, covalently immobilized antibiotics, which are most likely to be applied clinically, have demonstrated the ability to reduce bacterial colonization, biofilm formation, and implant-associated infections, potentially providing a novel and practical approach to reducing implant-associated infections (7–9). The covalent bonding of antibiotics to Ti surfaces has several advantages, including a reduced likelihood of development of bacterial resistance to the antibiotics compared with that for locally administered antibiotics and increased long-term stability (10).

An ideal antibacterial implant should combat a broad spectrum of bacteria, since implants may face multiple bacterial challenges when implanted *in vivo* (11). Vancomycin has been studied extensively as a candidate in the fabrication of antibacterial Ti implants (12). Vancomycin covalently tethered to Ti significantly inhibits bacterial colonization, while the recruitment, proliferation, differentiation, and maturation of osteoblasts remain unaffected (13, 14); in addition, it can prevent the development of *Staphylococcus aureus* resistance to rifampin *in vitro* (15). However, vancomycin has a limited ability to eradicate Gram-negative bacteria, such as *Escherichia coli* (7). To this end, tetracycline was investigated as a candidate in the fabrication of an antibacterial Ti implant to inhibit Gram-negative bacterial colonization (16). Unfortunately, it remains unclear whether the tetracycline modification is effective against Gram-positive pathogens, such as *Staphylococcus aureus* and *Staphylococcus epidermidis*.

Prior to the covalent attachment of antibacterial agents, the addition of a spacer on the Ti surface is necessary (14, 16). Flexible spacers allow the rapid movement and multiple orientations of bound antibacterial agents on the implant interface, which can promote peptide-bacterium interactions (17, 18). Polyethylene glycol (PEG) has been widely used for the chemical modification of biomaterials because of its nontoxic, nonantigenic, and nonimmunogenic properties (19, 20). Moreover, both the length of the PEG molecule and the functional group at the end of the PEG molecule can be altered as required, making PEG an attractive spacer for covalent antibiotic attachment to the Ti surface.

It should be emphasized that in orthopedic surgery, a significant increase in the incidence of complications because of antibiotic-resistant bacterial strains, such as methicillin-resistant *S. aureus* (MRSA), has been observed. Patients with MRSA infections have a poor prognosis, as such infections often have high recurrence rates and more sequelae than infections caused by methicillin-sensitive *S. aureus* strains (21). Therefore, the Ti implants should be fabricated specifically for prophylaxis against MRSA and other bacterial infections associated with the implants.

Enoxacin belongs to a class of fluoroquinolone antibiotics which can inhibit osteoclast formation and bone resorption. Enoxacin is able to prevent the binding of the B subunit of vacuolar $H^+$-ATPase (V-ATPase) and has been shown to have the potential to be able to counteract particle-induced bone implant osteolysis (22–25). Enoxacin can be bound to bisphosphonate to form bisenoxacin, which maintains the antibacterial capabilities of enoxacin and inhibits osteoclast formation (26, 27), indicating that the antibacterial properties of enoxacin are preserved even when it is covalently tethered to a molecule. Here, we examined the antibacterial properties of enoxacin-modified PEGylated titanium alloys against five bacterial strains, including *S. aureus*, *S. epidermidis*, methicillin-resistant *S. aureus*, methicillin-resistant *S. epidermidis* (MRSE), and *E. coli*, *in vitro* and *in vivo* to investigate its use for the prophylaxis of bacterial infections associated with the Ti implant.

## RESULTS

**MICs of enoxacin.** The MICs of enoxacin were 2 $\mu$g/ml for *S. aureus* and *S. epidermidis*, 4 $\mu$g/ml for MRSA, 0.5 $\mu$g/ml for MRSE, and 0.06 $\mu$g/ml for *E. coli*.

**Characterization of covalently immobilized enoxacin on Ti surface.** The reaction scheme for the synthesis of enoxacin bonded to Ti is shown in Fig. 1, and the covalent immobilization was confirmed by XPS following PEGylation of Ti, as shown in Fig. 2. PEG

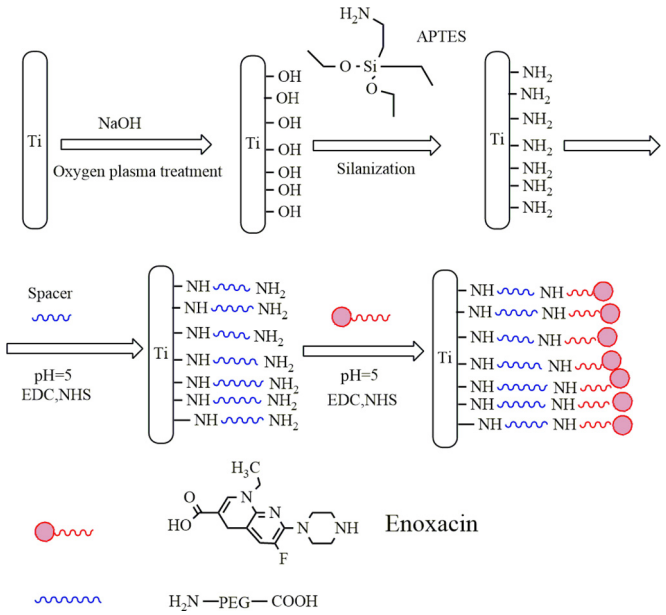


**FIG 1** Reaction scheme for the synthesis of enoxacin bonded to Ti and the surface treatments with Ti.

can be covalently bound to the amine-functionalized Ti (Ti-AA) surface through the reaction of —COOH and —$NH_2$ from PEG and Ti-AA, respectively, resulting in an amino bond. As indicated by X-ray photoelectron spectrometry (XPS), the native C1s spectrum of PEG-modified titanium (Ti-P) showed two peaks with binding energies of 287.7 and 285.3 eV, corresponding to C=O and O=C—N and to C—N, respectively, confirming amido bond formation after PEG immobilization. The spectrum taken after enoxacin immobilization onto the PEGylated Ti surface showed peaks at 288.1 and 285.4 eV, corresponding to C=O and O=C—N bonds and to the C—N bond, respectively. These peaks indicate that the amido bond was maintained on the Ti surface. Furthermore, the O1s, C1s, and N1s spectra were increased (Table 1), indicating that more C=O, O=C—N, and C—N bonds were formed, resulting in successful covalent immobilization of the enoxacin on the PEGylated Ti surface.

**Adhesion, proliferation, and morphology of hBMSCs.** The surface coating of an orthopedic implant should mitigate infection while maintaining the viability of human bone marrow mesenchymal stem cells (hBMSCs), which are critical in osteogenesis and bone implant osteointegration. We therefore evaluated the adhesion and proliferation of hBMSCs on the various Ti surfaces. As shown in Fig. 3A, cell adhesion was improved

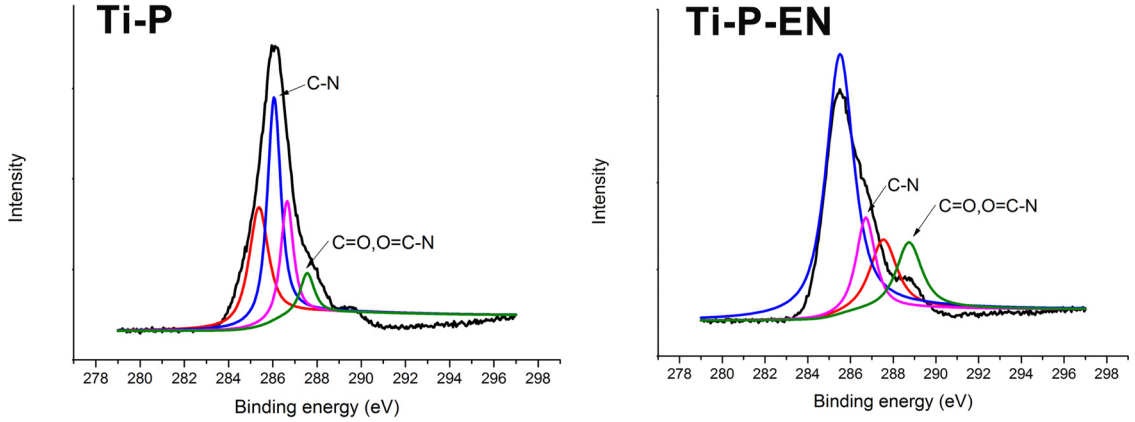


**FIG 2** XPS characterization of the enoxacin-modified PEGylated Ti surface.

**TABLE 1** Chemical composition and relative atomic ratios[a]

| | Atomic % | | |
|---|---|---|---|
| Atom | Ti | Ti-P | Ti-P-EN |
| C | 9.19 | 20.88 | 34.92 |
| N | 0.97 | 2.08 | 6.17 |
| O | 65.28 | 17.24 | 40.88 |
| Si | 4.77 | 6.38 | 4.81 |
| Ti | 17.92 | 2.94 | 13.23 |

[a]Abbreviations: Ti, titanium; Ti-P, PEG-modified titanium; Ti-P-EN, PEG- and enoxacin-modified titanium.

on Ti-P and enoxacin-modified Ti-P (Ti-P-EN) discs compared to that on the Ti control disc, while there was no significant difference in cell proliferation (Fig. 3B). These results indicate that coated Ti discs had no cytotoxic effects on either type of cell. After incubation for 24 h, the hBMSC actin cytoskeleton was visualized using Alexa Fluor 446 (red fluorescence), and the nuclei were stained with 4′,6-diamidino-2-phenylindole (DAPI; blue fluorescence). Cell spread was similar on all Ti discs (Fig. 3C).

**Protein adhesion.** The bovine serum albumin (BSA) concentration and absorbance (optical density at 562 nm [$OD_{562}$]) showed a positive linear correlation, described by the equation $y = 0.48x + 0.113$ ($r = 0.999$). At each time point, protein adhesion was significantly higher in the Ti group. Protein adhesion onto each Ti substrate peaked at 2 h. Compared with the inhibition of protein adhesion by Ti, PEGylated Ti and

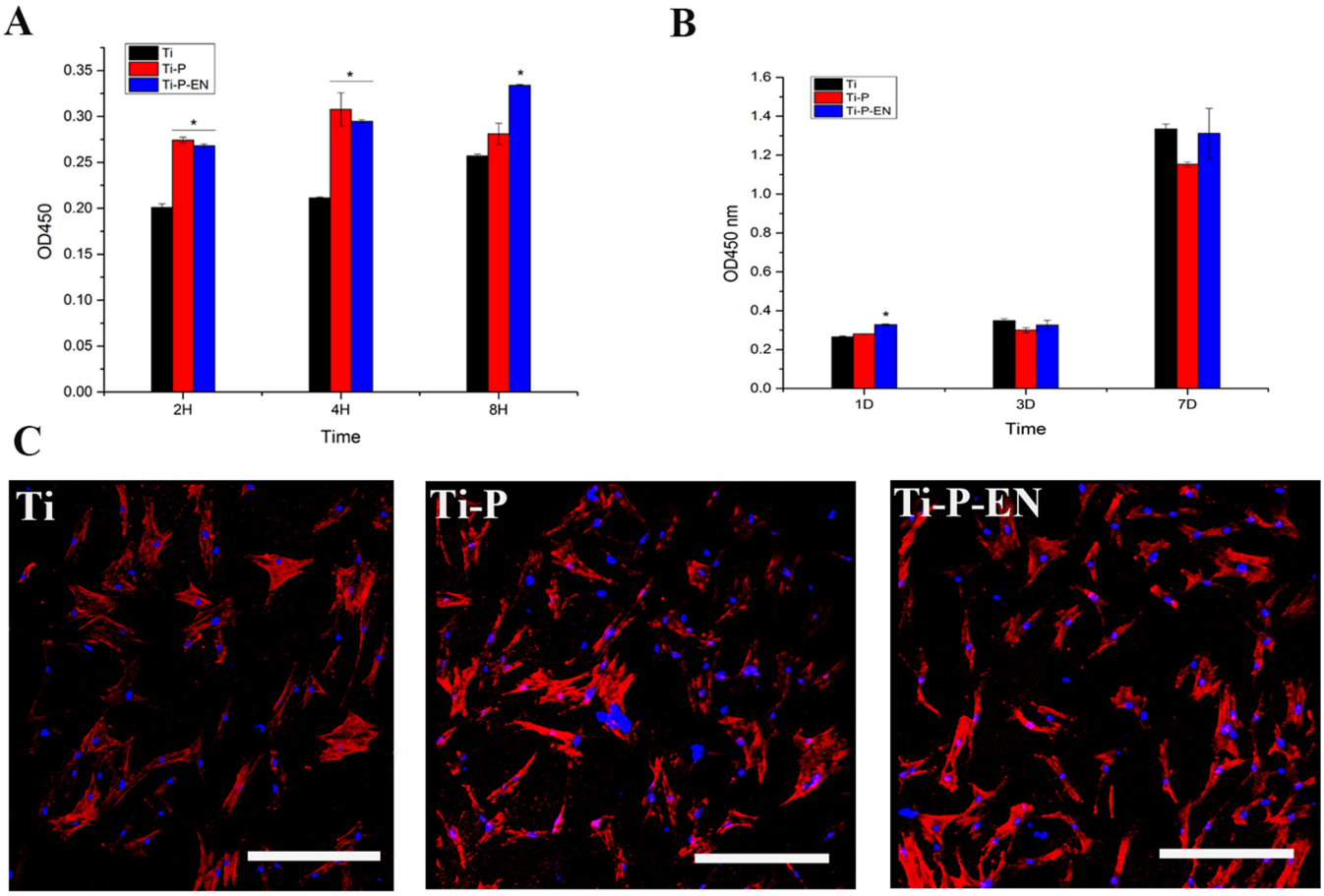


**FIG 3** (A and B) Adhesion and proliferation of hBMSCs onto the Ti samples, measured by the Cell Counting Kit-8 (CCK-8) assay at 2, 4, and 8 hours and 1, 3, and 7 days. *, $P < 0.05$. H, hours; D, days. (C) CLSM to characterize hBMSC morphology and spread onto the Ti surface at the same time points used for the assays whose results are presented in panels A and B. Cells plated on either control or enoxacin-modified surfaces for times out to 24 h showed no differences in morphology or number as a function of the surface modification. After 24 h of incubation, the hBMSC actin cytoskeleton was visualized by Alex Flour 446 staining (red fluorescence) and nuclei were stained with DAPI (blue fluorescence). Bar, 50 $\mu$m.

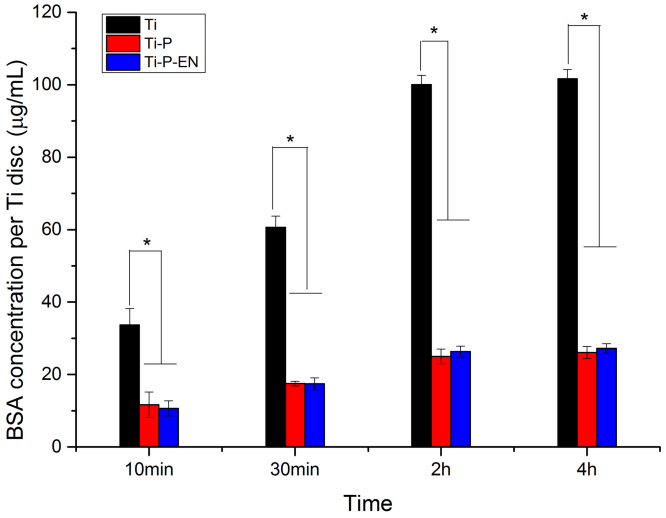


**FIG 4** Amount of BSA protein adsorption measured after 10 min, 30 min, 2 h, and 4 h of incubation of Ti, Ti-P, and Ti-P-EN with 1 ml of a BSA solution of 1 mg/ml. *, $P < 0.05$.

enoxacin-modified PEGylated Ti could significantly inhibit protein adhesion at each time point (Fig. 4).

**Characterization of bacterial colonization.** As shown in Fig. 5, the bacterial counts were normalized to log units, and the level of bacterial inhibition was normalized to the log reduction. Ti-P-EN could significantly inhibit colonization by various bacteria at each time point, while Ti and Ti-P did not demonstrate an antibacterial capacity. Compared to the counts for the control Ti group, the log reductions of *S. aureus*, MRSA, *S. epidermidis*, MRSE, and *E. coli* isolates were approximately 2.73, 3.10, 2.61, 2.69, and 1.61, respectively, at 6 h when the bacteria were cultured on Ti-P-EN and approximately 2.58, 2.53, 2.67, 2.17, and 1.56, respectively, at 24 h.

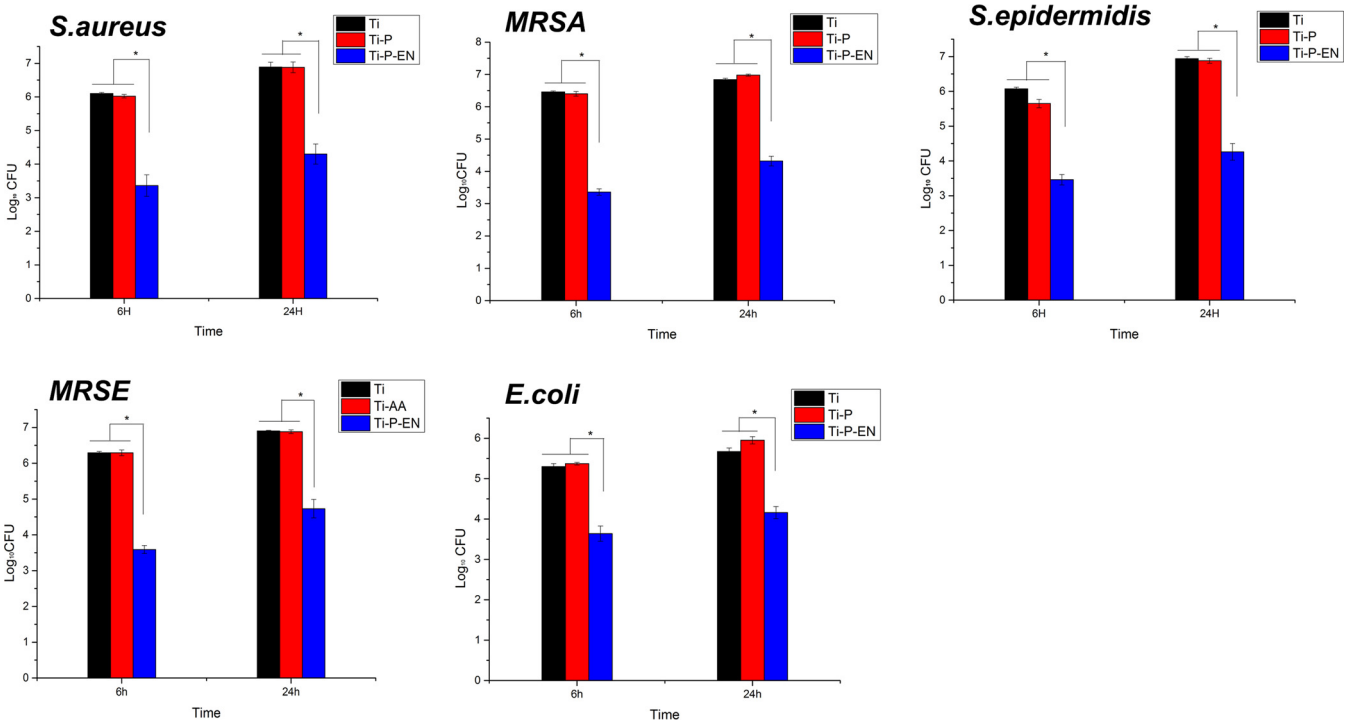


**FIG 5** Characterization of the level of bacterial colonization of the various Ti surfaces by the spread plate method. The CFU counts were normalized to log values. *, $P < 0.05$.

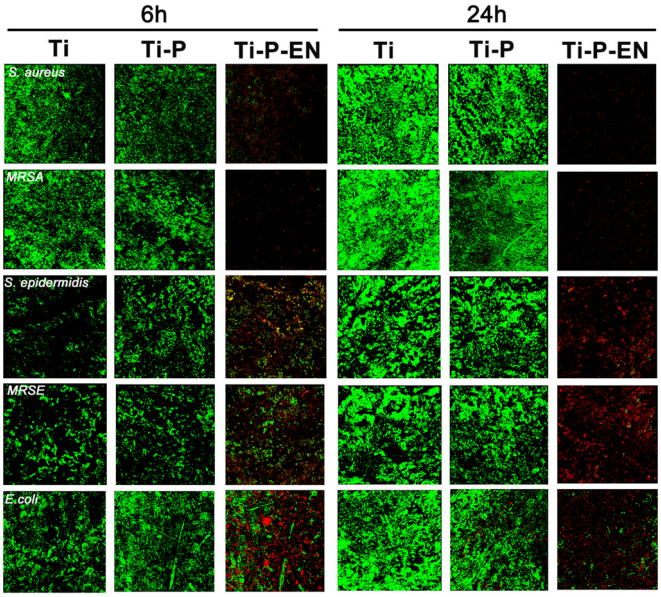


**FIG 6** The antibacterial properties of the samples after 6 h and 24 h of incubation with bacteria ($10^6$ CFU/ml) were evaluated by live/dead staining. Green, viable bacteria; red, dead bacteria.

**Confocal laser scanning microscopy (CLSM) and SEM to characterize bacterial adhesion and biofilm formation.** After 6 h and 24 h, each Ti substrate was incubated with bacteria (all strains mentioned above were used). Large numbers of bacterial colonies were apparent on the Ti control and the Ti-P groups at both time points. Fewer viable bacterial colonies were observed on the Ti-P-EN surface at 6 h and 24 h. Viable bacteria (stained green) were seen on the Ti and Ti-P substrates at 6 and 24 h (Fig. 6). Less green fluorescence was observed on the Ti-P-EN surface at both time points, while many dead bacteria (stained red) were observed on the Ti-P-EN surface. The amount of bacteria on each Ti sample was confirmed by scanning electron microscopy (SEM). Figure 7 shows that the Ti and Ti-P substrates had many adherent bacterial colonies

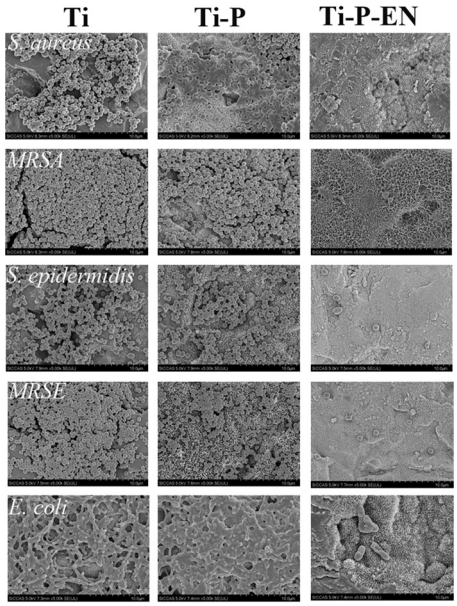


**FIG 7** SEM to characterize bacteria on the various Ti surfaces *in vitro* after 24 h of coculture.

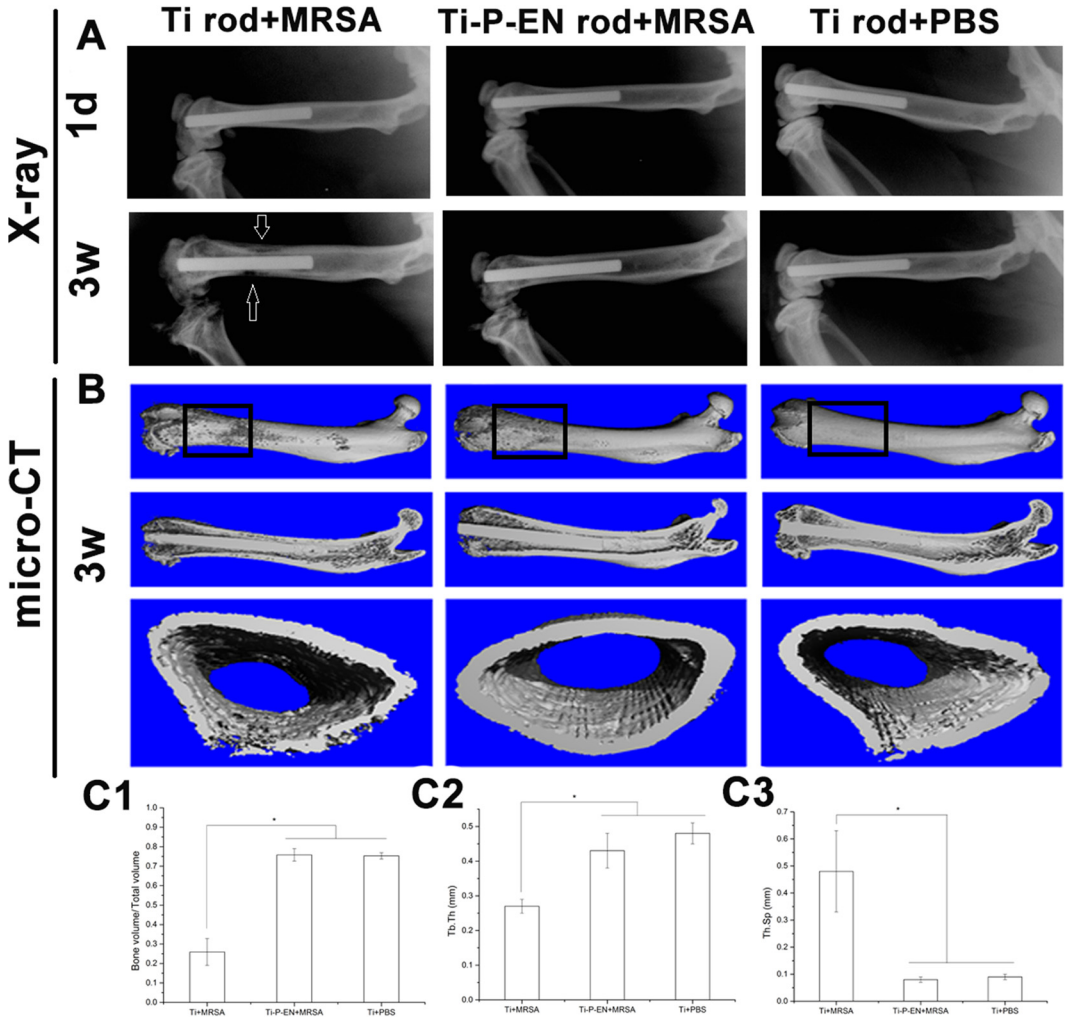


**FIG 8** *In vivo* study of Ti-P-EN antibacterial properties. X-ray images (A) and micro-CT results (B) of the femoral medullary cavity of rats into which a Ti rod was implanted obtained at 3 weeks after surgery and quantitative data for BV/TV (C1), Tb.Th (C2), and Tb.Sp (C3) obtained from the micro-CT analysis are shown. d, days; w, weeks. *, $P < 0.05$.

after 6 and 24 h, while the Ti-P-EN surface had very few adherent bacterial colonies at either time point.

***In vivo* prophylaxis of MRSA infection.** The enoxacin-functionalized Ti rods were successfully implanted in the femoral medullary cavity. No evident signs of cortical bone destruction were observed after 1 day (Fig. 8A). After 3 weeks, implant-related infection accompanied by low-density areas of cortical bone destruction was observed in the Ti control group (Fig. 8A). Micro-computed tomography (micro-CT) scans were obtained at 3 weeks postsurgery. As shown in Fig. 8B, osteolysis and absorption of cortical bone occurred around the Ti implant, while no signs of implant-related infection were observed in the Ti-P-EN group. For quantitative assessment, the volumes of the regions of interest (ROIs) obtained on the basis of the micro-CT scans are shown in Fig. 8. The rectangular frames in the three-dimensional (3-D) reconstructions of the micro-CT scans in Fig. 8B represent the ROIs. At 3 weeks after Ti and Ti-P-EN were contaminated with MRSA and implanted *in vivo*, the bone volume/total volume (BV/TV) and trabecular number were significantly higher, and the trabecular spacing was significantly lower in the Ti-P-EN group than in the Ti group (Fig. 8C1 to C3), indicating that the bone destruction was more serious in the Ti group.

**Quantitative determination of the Ti implant-related MRSA infection.** Clinical infection in the intramedullary cavity with a Ti implant was identified by yellow pus

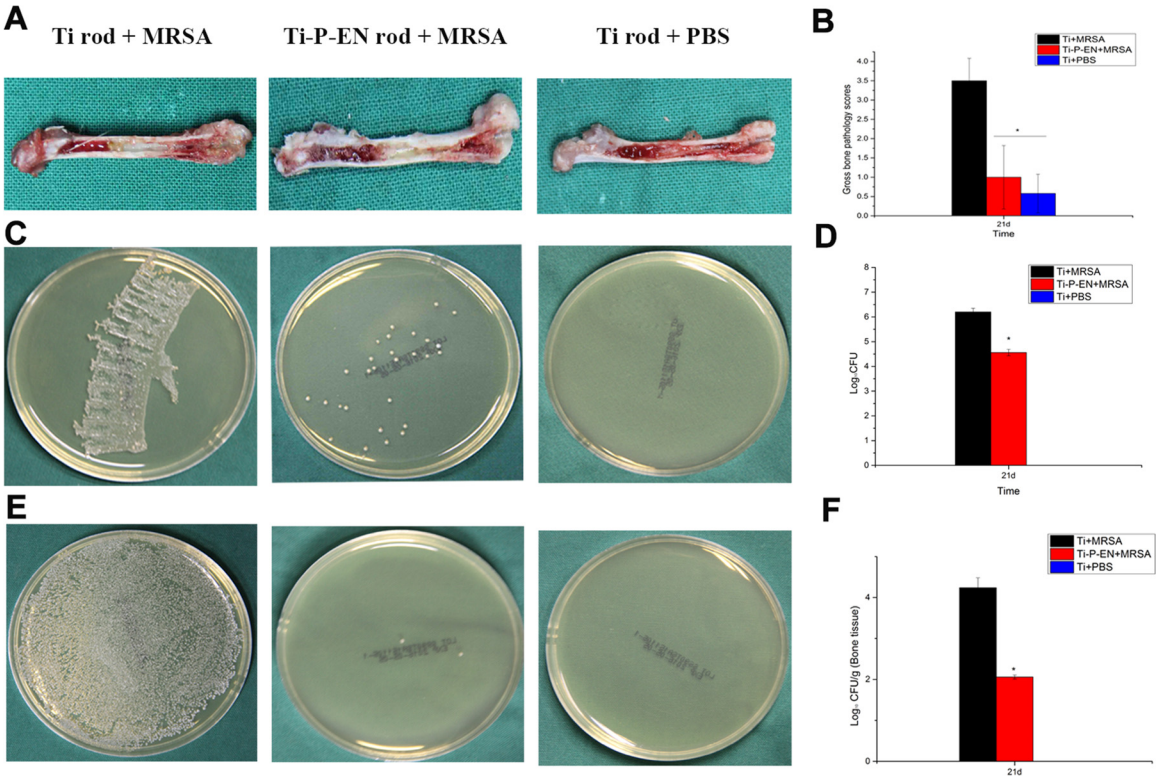


**FIG 9** Gross appearance and scores for longitudinal sections of the femurs of rats at the time of sacrifice and microbiological evaluation of the implants and bones. (A) Clinical signs of infection in the intramedullary cavity with a Ti implant are shown as yellow pus formation compared to the physiological appearance of the intramedullary cavity with a Ti implant without bacterial contamination after longitudinal sectioning of the femur. The femur implanted with Ti-P-EN appeared to be free of infection. (B) The *in vivo* efficacy of Ti-P-EN discs against MRSA was also investigated quantitatively. The scores for the Ti-P-EN group were significantly lower than those for the Ti groups. *, $P < 0.05$. (C and D) The spread plate method was used to characterize MRSA colonization on the control Ti and Ti-P-EN implants in a murine model of biomaterial-associated infection by counting of the number of CFU. (E and F) The spread plate method was used to quantify the MRSA bacteria located in the tissue surrounding the control Ti and Ti-P-EN implants. The bacterial counts were normalized to log values. All data represent means ± standard errors of the means from three independent experiments. *, $P < 0.05$.

formation compared to the normal physiological appearance with a Ti implant (Fig. 9A) after longitudinal sectioning of the femur. Bone lesions, periosteal reactions, and bone structural abnormalities were also observed. The mean pathological scores for each longitudinal section of the femora into which the various Ti rods were implanted were 3.5 ± 0.58, 1.0 ± 0.82, and 0.58 ± 0.5 for the group with a Ti implant infected with MRSA (the Ti+MRSA group), the group with a Ti-P-EN implant infected with MRSA (the Ti-P-EN+MRSA group), and the group with a Ti implant treated with phosphate-buffered saline (PBS) (the Ti+PBS group) (Fig. 9B), respectively. There was no significant difference between the scores for the Ti-P-EN+MRSA and Ti+PBS groups ($P > 0.05$). Compared with the average score for the Ti+MRSA group, the average score for the Ti-P-EN+MRSA group significantly decreased ($P < 0.05$). The amount of bacteria dwelling on the Ti-P-EN rod was significantly smaller than that dwelling on the Ti rod (Fig. 9C). Compared with the bacterial count on the rod in the Ti group, the bacterial count on the rod in the Ti-P-EN group was reduced by 1.64 log units (Fig. 9D). The amount of bacteria dwelling on the bone tissue around the rod for the Ti-P-EN group was significantly smaller than that for the Ti group (Fig. 9E). The log reduction in the amount of Ti-P-EN in the bone tissue around the Ti rod was 2.17 (Fig. 9F).

**SEM characterization and histological analysis.** SEM images showed spherical bacterial growth on the Ti rods and the surrounding bone tissue, whereas no spherical bacteria were detected on the enoxacin-modified Ti rods or the surrounding bone tissue (Fig. 10). Hematoxylin and eosin (H&E) staining was used for histological analysis. After 3 weeks, the control Ti implants showed bone resorption around the materials,

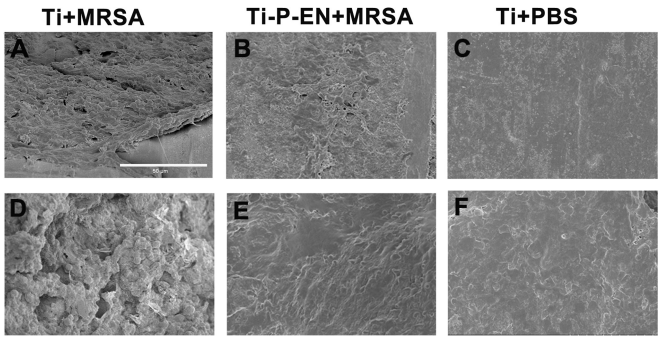


**FIG 10** SEM characterization of the bacteria on the Ti rod and enoxacin-modified Ti rod. SEM images showed spherical bacterial growth on the Ti rod and the surrounding bone tissue (A and D), while no spherical bacteria were detected on the enoxacin-modified titanium rod or the surrounding bone tissue (B, C, E, and F). Bar, 50 $\mu$m.

and inflammation was observed at the site of absorbed bone (Fig. 11). In contrast, no bone resorption was observed around the enoxacin-modified Ti implant, and the surrounding bone retained its integrity, similar to the findings for the negative control.

## DISCUSSION

Infection related to orthopedic implants is one of the most common complications of orthopedic surgery and has serious consequences (28). There are two main reasons why Ti implants are susceptible to infection: it is easy for the bacteria to adhere to the implant surface and form biofilms, and unfortunately, the immune capability of the implant/tissue interface is poor (29). Currently, two main approaches for biofunctionalizing Ti to obtain bactericidal properties, passive and active approaches, exist, depending on whether the Ti implant surface can locally deliver antibacterial agents. A passive antibacterial Ti surface can inhibit bacterial adhesion or kill bacteria when they contact the surface. In contrast, an active antibacterial Ti surface can locally release antibacterial agents and kill the bacteria around the Ti implant (30). The passive implant coating involves the development of a bactericidal implant surface, which plays a crucial role in the antibacterial activity of the implant (31). In the current study, we fabricated a passive antibacterial Ti surface in which enoxacin was covalently immobilized onto the PEGylated surface to achieve antibacterial activity without affecting hBMSC adhesion or proliferation.

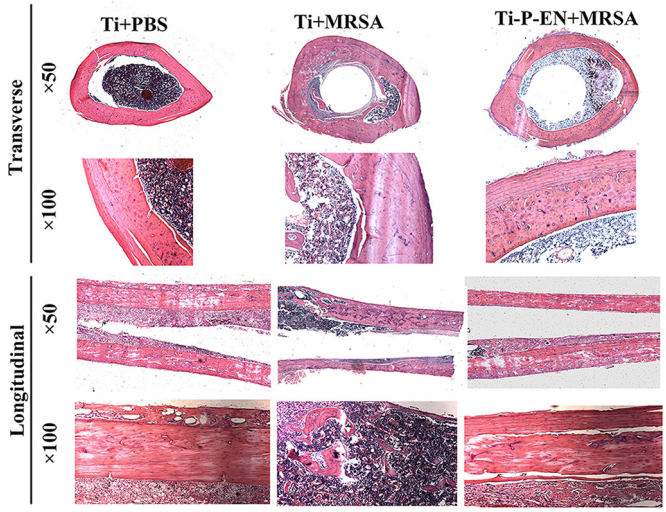


**FIG 11** H&E staining of decalcified femur bones around the Ti rod *in vivo*. Bone absorption formed in the Ti+MRSA group, and significant inflammation was observed.

In order to evaluate the broad-spectrum antibacterial activity of the PEGylated and the enoxacin-modified Ti, the most common Gram-positive and Gram-negative bacterial strains in orthopedic implant infections were selected (28). The *in vitro* antibacterial assay demonstrated that the enoxacin tethered onto the PEGylated Ti surface could maintain its antibacterial activity and was able to reduce the adhesion and biofilm formation of both Gram-negative and Gram-positive bacterial strains. Strikingly, the enoxacin tethered onto the PEGylated Ti rod could prevent the implant-associated infection caused by MRSA in the rat model over 3 weeks. The MRSA count on Ti-P-EN discs was reduced by 1.64 log units compared to that on Ti discs, demonstrating the clinical potential of such coatings to resist MRSA or other bacterial contamination. The potential mechanism of the prophylactic efficacy of the enoxacin-bonded titanium observed in this study may be divided into two parts, including the antiadhesive property at the early stage, because the bacteria were killed on contact, and the flexible PEG spacers (17), which allowed the enoxacin to react with the bacteria and clear the bacteria adhering to the implant surface.

Surface functionalization with a functional group is the first step in the covalent attachment of antibiotics and biomolecules onto the Ti surface. Ti silanized with 3-aminopropyltriethoxysilane (APTES) forms three siloxy bonds (Ti—O—Si—) with the Ti-oxide surface and exposes a primary amine group for further chemical covalent reactions (31–33). Enoxacin is effective against many Gram-positive and Gram-negative bacteria by interfering with the DNA replication of the bacteria. It can inhibit bacterial DNA gyrase and topoisomerase IV, which prevents bacterial DNA replication, transcription, repair, and recombination (34). A spacer is always needed prior to the covalent attachment of antibiotics to a Ti surface (5) and serves as a bridge that links antibacterial agents to the implant surface, making the orientation of antibacterial agents more flexible. PEG has been widely used as a spacer because of its nontoxicity and its functional group, which may be easily modified to link to various bioactive molecules and antibacterial agents (35). In the current study, the PEG molecules could extend enoxacin away from the Ti surface, allowing enoxacin to enter the bacterial cell wall and bind to the bacterium's DNA gyrase and topoisomerase IV. In addition, after implantation plasma proteins are recruited to the implant surface and form a plasma layer, which can disable the antibacterial coating surface (36); however, PEG has the ability to inhibit protein binding and avoids the adverse effects described above (37–39), and this function has also been proved by the current study. Our previous study demonstrated that the covalent cross-linking under the action of 1-ethyl-3-(3-dimethylaminopropyl) carbodiimide (EDC) and *N*-hydroxysuccinimide (NHS) enhanced the stability of the coating, in contrast to that of the controlled-release system (40). Hickok and Shapiro also reported that the covalently tethered antibacterial layer could resist bacterial colonization over the long term (months to years) (7). Our *in vivo* study also showed that the antibacterial effect of enoxacin tethered on the PEGylated Ti could be preserved, which indirectly demonstrated the stability of the covalently tethered antibacterial layer.

While surfaces to which antibiotics are tethered have demonstrated promise for the potential inhibition of bacterial colonization, it is important to examine if such coated discs affect the growth of hBMSCs, which are an important cell type in bone tissue turnover and regeneration processes (8). One of the disadvantages of antibiotics covalently immobilized on Ti surfaces is that they inhibit hBMSC adhesion and proliferation, and multiple biomolecules must be coimmobilized on the Ti surfaces to achieve multiple biofunctions in order to avoid the disadvantage described above (41). In our *in vitro* study, no visible differences in the morphology, size, and density of adherent cells were observed among osteoblast-like cells cultured on the control or the enoxacin-tethered Ti implant surfaces. Furthermore, the covalent modification of the Ti surfaces does not allow the release of any antibiotic; thus, it does not cause bacterial resistance due to the administration of excessive amounts of antibiotic.

Taken together, our *in vitro* and *in vivo* studies demonstrated that the enoxacin tethered on the PEGylated Ti surface could decrease the levels of Gram-positive and

Gram-negative bacterial colonization and biofilm formation without affecting hBMSC adhesion and proliferation and could prevent MRSA-related Ti implant infections *in vivo*.

**Conclusion.** In this study, enoxacin was covalently immobilized on a PEGylated Ti surface. The PEG acted as a flexible spacer, which would enhance the interaction of enoxacin with the bacteria. In addition, the PEGylated Ti could improve the cytocompatibility of the implant. The enoxacin-functionalized Ti is potentially more useful than the vancomycin-functionalized Ti, as it effectively prevented both Gram-positive and Gram-negative bacterial colonization. When hBMSCs were cultured on surfaces to which enoxacin was tethered, there was little change in the morphology, size, or density of adherent cells. Based on the findings of these studies, we predict that the surfaces preserve cell commitment, differentiation, and proliferative status while maintaining the osseointegrative capacity of the modified implant *in vivo*. Our data demonstrate that the Ti implants to which enoxacin is tethered have the potential to effectively prevent infections caused by multiple bacterial species while maintaining the excellent biocompatibility of the Ti *in vivo*.

## MATERIALS AND METHODS

**Materials.** Ti6Al4V (titanium [Ti] alloy; 10 mm in diameter and 2 mm in thickness) and Ti6Al4V rods (for the *in vivo* study, 1.5 mm in diameter and 20 mm in height) were obtained from Shanghai Yan Ti Metal Material Co. Ltd. Enoxacin and 4′,6′-diamidino-2-phenylindole (DAPI) were obtained from Sigma-Aldrich. Tryptic soy broth (TSB) and bovine serum albumin (BSA) were purchased from Beyotime Biotechnology (China), whereas LIVE/DEAD BacLight bacterial viability kits were from Molecular Probes. Polyethylene glycol (3.4 kDa) was obtained from (JenKem Technology, Beijing, China), 3-aminopropyltriethoxysilane (APTES) was obtained from Sinopharm Chemical Reagent Co. (China), 1-ethyl-3-(3-dimethylaminopropyl) carbodiimide (EDC) was from Tokyo Chemical Industry Co., Ltd. (Tokyo, Japan), and *N*-hydroxysulfosuccinimide (sulfo-NHS) was from Shanghai Sinopharm Chemical Reagent Co. (Shanghai, China). $\alpha$ modified Eagle's medium ($\alpha$-MEM) was from Gibco (Paisley, UK), fetal bovine serum (FBS) was from Gibco (Australia), and rhodamine phalloidin (from *Amanita phalloides*), *Staphylococcus aureus* (ATCC 25923), methicillin-resistant *Staphylococcus aureus* (MRSA; ATCC 43300), *Staphylococcus epidermidis* (ATCC 35984), methicillin-resistant *Staphylococcus epidermidis* (MRSE; ATCC 287), and *Escherichia coli* (ATCC 25922) were obtained from ATCC.

**Methods. (i) Determination of MIC of enoxacin.** The *S. aureus* (ATCC 25923), MRSA (ATCC 43300), *S. epidermidis* (ATCC 35984), MRSE (ATCC), and *E. coli* (ATCC 25922) bacterial strains were cultured overnight in TSB. The bacteria were then resuspended in sterile TSB to approximately $1 \times 10^5$ CFU/ml. Next, they were seeded at $10^5$ CFU/ml in flat-bottom 96-well plates with serial dilutions of enoxacin (concentration range, 512 $\mu$g/ml to 0.125 $\mu$g/ml) in TSB and incubated for 24 h at 37°C. The MIC was defined as the minimum concentration of enoxacin that inhibited bacterial growth.

**(ii) Covalent immobilization and characterization of enoxacin on PEGylated Ti surfaces.** A Ti disk (10 mm in diameter by 2 mm) was treated with NaOH to introduce a functional hydroxyl group on the Ti surface. After it was dried under vacuum, the NaOH-etched Ti disk was silanized with 10 wt% APTES in toluene solution at 100°C for 12 h to introduce an amine group on the Ti surface. Afterwards, the amine-functionalized Ti (Ti-AA) was soaked in PEG solution (1 mg/ml) and oscillated for 8 h at 37°C under EDC and NHS. The PEGylated titanium was soaked in enoxacin (1 mg/ml) and was oscillated for 8 h at 37°C with carbodiimide and *N*-hydroxysulfosuccinimide to yield PEGylated titanium with covalently conjugated enoxacin (Fig. 1). The surface was washed with PBS to detach any excess enoxacin. This composite was denoted Ti-P-EN. The successful covalent immobilization of enoxacin on Ti surfaces was characterized by X-ray photoelectron spectroscopy (XPS).

**(iii) hBMSC adhesion and proliferation assays and morphological analyses on Ti surfaces.** The study was approved by the Ethical Committee of the Shanghai Ninth People's Hospital, Shanghai Jiao Tong University School of Medicine, Shanghai, China. Human bone marrow mesenchymal stem cells (hBMSCs) were cultured to near confluence in $\alpha$-MEM containing 10% fetal bovine serum at 37°C in 5% $CO_2$. At passage 3, the hBMSCs were harvested using a digestion reagent containing 0.25% trypsin and 0.02% EDTA and were resuspended in $\alpha$-MEM. Harvested cells were seeded at a concentration of $1 \times 10^5$ cells/ml onto Ti samples that had been placed in 24-well plates. The cells were cultured at 37°C in 5% $CO_2$. hBMSC adhesion and proliferation were evaluated at 2 h, 4 h, 8 h, 1 days, 3 days, and 7 days after seeding. At 1 day after seeding, Ti substrates were fixed with 4% paraformaldehyde, and confocal laser scanning microscopy (CLSM) was used to characterize the cytoskeletal morphology with DAPI and rhodamine phalloidin as described in a previous study (42).

**(iv) Antiprotein adhesion assay on various Ti substrates.** An antiprotein adhesion assay on various Ti substrates (Ti, Ti-P, and Ti-P-EN) was performed using bovine serum albumin (BSA). The Ti substrates were incubated in 1 mg/ml BSA at 37°C, and the $OD_{562}$ was taken at 10 min, 30 min, 2 h, and 4 h. The amount of BSA in each sample was determined using a standard curve of the BSA concentration against the $OD_{562}$ according to the manufacturer's instructions (Beyotime Biotechnology, Shanghai, China).

**Antibacterial assays. (i) Spread plate method.** Biomaterials often have the risk of colonization by various Gram-positive and Gram-negative bacteria in the human body. In the present study, five bacterial

**TABLE 2** Animal experimental groups[a]

| Group | No. of rats undergoing the following analysis or procedure: | | | |
|---|---|---|---|---|
| | Total | Pathological score and spread plate method | Micro-CT | SEM characterization and histological analysis |
| Ti rod + MRSA | 12 | 5 | 5 | 2 |
| Ti-P-EN rod + MRSA | 12 | 5 | 5 | 2 |
| Ti rod + PBS | 12 | 5 | 5 | 2 |

[a]Abbreviations: Ti, titanium; Ti-P-EN, enoxacin- and PEG-modified titanium; MRSA, methicillin-resistant *Staphylococcus aureus*; PBS, phosphate-buffered saline; micro-CT, micro-computed tomography; SEM, scanning electron microscopy.

strains, comprising *S. aureus*, MRSA, *S. epidermidis*, MRSE, and *E. coli*, were employed to investigate the antimicrobial properties of the Ti implants. Three types of Ti implants were used in the experiment: control unmodified Ti (the Ti group), PEG-functionalized Ti (the Ti-P group), and Ti-P to which was enoxacin covalently tethered onto the PEG (the Ti-P-EN group). Each of the five bacterial species was resuspended to a concentration of $1 \times 10^6$ CFU/ml. Each Ti substrate was incubated with 1 ml of bacterial suspension ($1 \times 10^6$ CFU/ml) at 37°C in 24-well plates. After incubations for 6 h and 24 h, the spread plate method was used to detect viable bacteria and characterize the bacterial growth on each Ti surface. Adherent bacteria were detached by cleaning the discs with ultrasonication for 20 min in a 150-W ultrasonic bath in 1 ml phosphate-buffered saline (PBS). The bacteria were then seeded onto agar plates using serial dilutions. The plates were incubated at 37°C for 24 h, and the resulting bacterial colonies were counted.

**(ii) CLSM.** After 6 h and 24 h of bacterial coculture with each Ti substrate (all strains mentioned above were used), the Ti discs were removed. They were gently washed three times with PBS and fixed with 4% paraformaldehyde for 1 h. The viability of the bacteria on the Ti discs was characterized using LIVE/DEAD BacLight bacterial viability kits, and the bacteria were analyzed with a confocal laser scanning microscope (model TCS SP2; Leica, Germany). The viable and nonviable bacteria were distinguished by color: the viable bacteria fluoresced green, while the nonviable bacteria with damaged membranes fluoresced red.

**(iii) SEM.** For SEM characterization, the Ti discs were fixed overnight in 2.5% glutaraldehyde. Each Ti sample was dehydrated through a series of graded ethanol solutions (30, 50, 70, 80, 90, 100, and 100%) for 10 minutes. The samples were subsequently freeze-dried, sputter coated with platinum, and observed using a scanning electron microscope (model JSM-6700F; JEOL, Japan).

***In vivo* study of antibacterial properties of Ti-P-EN. (i) X-ray analysis to evaluate the extent of cortical bone destruction.** To assess the antibacterial ability of Ti to which enoxacin was covalently tethered *in vivo*, modified implants were inserted into rat femurs. The experiment was approved by the Animal Experimentation Ethical Committee of the Shanghai Ninth People's Hospital, Shanghai Jiao Tong University School of Medicine (approval 2014-68). The Ti implant samples were shaped into rods of 1.5 mm in diameter and 20 mm in height. The Ti rod samples were denoted Ti rods, and the enoxacin-modified Ti rods were denoted Ti-P-EN rods. The Ti and Ti-P-EN rod samples were implanted in the femur via the femoral condyles. Briefly, 36 12-week-old female Sprague-Dawley (SD) rats (weight, 399.0 ± 8.94 g) were used and randomly assigned to one of three groups (Table 2). Intraperitoneal injection of pentobarbital sodium (30 mg/kg of body weight) was used for anesthesia. After analgesia, the senior orthopedic surgeons (Bing Yue and Teng Long) performed the animal surgeries. The knee of the rat was opened to expose the condyles, and the bone cavity was expanded with electroporation until it was large enough to hold the Ti rod. Prior to *in vivo* implantation, the Ti implants were contaminated with MRSA by soaking the Ti rods and Ti-P-EN rods in a bacterial solution ($1 \times 10^8$ CFU/ml) for 2 min. The rods were gently washed and implanted into the femur. Ti rods soaked in PBS acted as a negative control. After 1 day and 3 weeks, X-ray scans were carried out to evaluate the destruction of cortical bone.

**(ii) Quantitative analysis of bacterial growth on the Ti rod and in surrounding bone tissue.** After 3 weeks, the rats were sacrificed by cervical dislocation and the femurs were harvested. Gross bone pathology scores were determined by use of the following criteria: a score of 0 indicated no local abscess, sequestrum formation, reactive bone formation, or red skin coloration; a score of 1 indicated red skin coloration but no local abscess, sequestrum formation, or reactive bone formation; a score of 2 indicated enlargement of the bone marrow cavity and reactive new bone formation; a score of 3 indicated local abscess formation, periosteal reaction, purulent secretions, or sinus formation; and a score of 4 indicated severe bone resorption, abscess formation, and extension to the backbone (43).

The numbers of CFU of bacteria on Ti rods and surrounding bone tissue were determined by a spread plate method. After 3 weeks, the rats were sacrificed, the Ti rods were removed under sterile conditions, and the surrounding bone tissue was ground. A spread plate method was used to quantitatively determine the number of bacterial CFU on the Ti rod and the surrounding bone tissue. The Ti rods were detached by sonication in a 150-W ultrasonic bath for 20 min in 1 ml PBS, and the crushed bones were placed in 1 ml PBS. The numbers of bacterial CFU on the Ti rod and bone tissue were determined by serial dilution on agar plates. After inoculation, the agar plates were incubated at 37°C for 24 h, and the resulting colonies were counted. SEM was used to further characterize the bacterial colonization on the Ti rod *in vivo*.

**(iii) Micro-computed tomography.** The harvested femurs were then evaluated using a high-resolution micro-CT (model Skyscan 1072; Skyscan, Aartselaar, Belgium) to assess cortical bone destruc-

tion around the implants ($n = 5$ femurs per group). Scanning was performed at an isometric resolution of 20 $\mu$m and at X-ray energy settings of 80 kV and 80 mA. After the two (2-D) and three-dimensional (3-D) views of the implant with the surrounding new bone were reconstructed, a square region of interest (ROI) around the midline suture was selected for further qualitative and quantitative analysis. The bone volume/total volume (BV/TV), the mean trabecular thickness (Tb.Th), and the mean trabecular separation (Tb.Sp) were obtained.

**(iv) SEM and histological analysis of the bone tissue around the Ti rod.** SEM was used to characterize bacterial colonization on the Ti rod and surrounding bone tissue. Samples were prepared for SEM as described above. For histological analysis, the femurs containing Ti rods were fixed in 4% paraformaldehyde overnight and then decalcified in 10% EDTA for 2 weeks using ultrasound. The decalcified femur bones were used for hematoxylin and eosin (H&E) staining to characterize the bone destruction and inflammation around the Ti rod.

**Statistical analysis.** All data are expressed as the mean ± standard deviation for continuous variables. One-way analysis of variance (ANOVA) was performed, and confidence intervals were determined using SPSS software, followed by the Student Newman-Keuls (S-N-K) test to evaluate the differences between groups. *P* values of less than 0.05 were considered statistically significant.

## ACKNOWLEDGMENTS

This research was supported by the National Natural Science Foundation of China (81472119, 81501856, 81501855, and 81672196), Shanghai Municipal Education Commission-Gaofeng Clinical Medicine grant support (20161423), the National High-Tech Research and Development Program (863 Program) of China (2014AA020539), and the Shanghai Sailing Program (15YF1407000).

B.N., T.L., and H.A. carried out the experiments. B.N. prepared the manuscript. B.Y. designed the experiments. B.Y., J.Z., and T.T. revised the manuscript. All authors reviewed the manuscript.

## REFERENCES

1. Liu X, Chu PK, Ding C. 2004. Surface modification of titanium, titanium alloys, and related materials for biomedical applications. Mater Sci Eng R Rep 47:49–121. https://doi.org/10.1016/j.mser.2004.11.001.
2. Ferraris S, Spriano S. 2016. Antibacterial titanium surfaces for medical implants. Mater Sci Eng C 61:965–978. https://doi.org/10.1016/j.msec.2015.12.062.
3. Zhao L, Chu PK, Zhang Y, Wu Z. 2009. Antibacterial coatings on titanium implants. J Biomed Mater Res B Appl Biomater 91:470–480. https://doi.org/10.1002/jbm.b.31463.
4. Nie B, Ao H, Chen C, Xie K, Zhou J, Long T, Tang T, Yue B. 2016. Covalent immobilization of KR-12 peptide onto a titanium surface for decreasing infection and promoting osteogenic differentiation. RSC Adv 6:46733–46743. https://doi.org/10.1039/C6RA06778F.
5. Costa F, Carvalho IF, Montelaro RC, Gomes P, Martins MCL. 2011. Covalent immobilization of antimicrobial peptides (AMPs) onto biomaterial surfaces. Acta Biomater 7:1431–1440. https://doi.org/10.1016/j.actbio.2010.11.005.
6. Kuehl R, Brunetto PS, Woischnig AK, Varisco M, Rajacic Z, Vosbeck J, Terracciano L, Fromm KM, Khanna N. 2016. Preventing implant-associated infections by silver coating. Antimicrob Agents Chemother 60:2467–2475. https://doi.org/10.1128/AAC.02934-15.
7. Hickok NJ, Shapiro IM. 2012. Immobilized antibiotics to prevent orthopaedic implant infections. Adv Drug Deliv Rev 64:1165–1176. https://doi.org/10.1016/j.addr.2012.03.015.
8. Kucharíková S, Gerits E, De Brucker K, Braem A, Ceh K, Majdič G, Spanič T, Pogorevc E, Verstraeten N, Tournu H, Delattin N, Impellizzeri F, Erdtmann M, Krona A, Lövenklev M, Knezevic M, Fröhlich M, Vleugels J, Fauvart M, de Silva WJ, Vandamme K, Garcia-Forgas J, Cammue BPA, Michiels J, Van Dijck P, Thevissen K. 2015. Covalent immobilization of antimicrobial agents on titanium prevents Staphylococcus aureus and Candida albicans colonization and biofilm formation. J Antimicrob Chemother 71:936–945. https://doi.org/10.1093/jac/dkv437.
9. Shapiro IM, Hickok NJ, Parvizi J, Stewart S, Schaer TP. 2012. Molecular engineering of an orthopaedic implant: from bench to bedside. Eur Cell Mater 23:362–370.
10. Hickok NJ, Ketonis C, Adams CS. 2011. Tethered antibiotics A2, p 281–294. *In* Ducheyne P (ed), Comprehensive biomaterials. Elsevier, Oxford, United Kingdom.
11. Jin G, Qin H, Cao H, Qiao Y, Zhao Y, Peng X, Zhang X, Liu X, Chu PK. 2015. Zn/Ag micro-galvanic couples formed on titanium and osseointegration effects in the presence of S. aureus. Biomaterials 65:22–31. https://doi.org/10.1016/j.biomaterials.2015.06.040.
12. Antoci V, Jr, Adams CS, Hickok NJ, Shapiro IM, Parvizi J. 2007. Vancomycin bound to Ti rods reduces periprosthetic infection: preliminary study. Clin Orthop Relat Res 461:88–95.
13. Jose B, Antoci V, Jr, Zeiger AR, Wickstrom E, Hickok NJ. 2005. Vancomycin covalently bonded to titanium beads kills Staphylococcus aureus. Chem Biol 12:1041–1048.
14. Edupuganti OP, Antoci V, Jr, King SB, Jose B, Adams CS, Parvizi J, Shapiro IM, Zeiger AR, Hickok NJ, Wickstrom E. 2007. Covalent bonding of vancomycin to Ti6Al4V alloy pins provides long-term inhibition of Staphylococcus aureus colonization. Bioorg Med Chem Lett 17:2692–2696. https://doi.org/10.1016/j.bmcl.2007.03.005.
15. Rottman M, Goldberg J, Hacking SA. 2012. Titanium-tethered vancomycin prevents resistance to rifampicin in Staphylococcus aureus in vitro. PLoS One 7:e52883. https://doi.org/10.1371/journal.pone.0052883.
16. Davidson H, Poon M, Saunders R, Shapiro IM, Hickok NJ, Adams CS. 2015. Tetracycline tethered to titanium inhibits colonization by Gram-negative bacteria. J Biomed Mater Res B Appl Biomater 103:1381–1389. https://doi.org/10.1002/jbm.b.33310.
17. Onaizi SA, Leong SSJ. 2011. Tethering antimicrobial peptides: current status and potential challenges. Biotechnol Adv 29:67–74. https://doi.org/10.1016/j.biotechadv.2010.08.012.
18. Bagheri M, Beyermann M, Dathe M. 2009. Immobilization reduces the activity of surface-bound cationic antimicrobial peptides with no influence upon the activity spectrum. Antimicrob Agents Chemother 53:1132–1141. https://doi.org/10.1128/AAC.01254-08.
19. Zhou J, Nie B, Zhu Z, Ding J, Yang W, Shi J, Dong X, Xu J, Dong N. 2015. Promoting endothelialization on decellularized porcine aortic valve by immobilizing branched polyethylene glycol modified with cyclic-RGD peptide: an in vitro study. Biomed Mater 10:065014. https://doi.org/10.1088/1748-6041/10/6/065014.
20. Zhou J, Hu S, Ding J, Xu J, Shi J, Dong N. 2013. Tissue engineering of heart valves: PEGylation of decellularized porcine aortic valve as a scaffold for in vitro recellularization. Biomed Eng Online 12:87. https://doi.org/10.1186/1475-925X-12-87.
21. Teterycz D, Ferry T, Lew D, Stern R, Assal M, Hoffmeyer P, Bernard L, Uçkay I. 2010. Outcome of orthopedic implant infections due to different staphylococci. Int J Infect Dis 14:e913–e918. https://doi.org/10.1016/j.ijid.2010.05.014.

22. Kartner N, Manolson MF. 2014. Novel techniques in the development of osteoporosis drug therapy: the osteoclast ruffled-border vacuolar $H^+$-ATPase as an emerging target. Expert Opin Drug Discov 9:505–522. https://doi.org/10.1517/17460441.2014.902155.
23. Liu XQ, Qu XH, Wu CL, Zhai ZJ, Tian B, Li HW, Ouyang ZX, Xu XC, Wang WG, Fan QM, Tang TT, Qin A, Dai KR. 2014. The effect of enoxacin on osteoclastogenesis and reduction of titanium particle-induced osteolysis via suppression of JNK signaling pathway. Biomaterials 35:5721–5730. https://doi.org/10.1016/j.biomaterials.2014.04.006.
24. Ostrov DA, Magis AT, Wronski TJ, Chan EKL, Toro EJ, Donatelli RE, Sajek K, Haroun IN, Nagib MI, Piedrahita A, Harris A, Holliday LS. 2009. Identification of enoxacin as an inhibitor of osteoclast formation and bone resorption by structure-based virtual screening. J Med Chem 52:5144–5151. https://doi.org/10.1021/jm900277z.
25. Toro EJ, Zuo J, Ostrov DA, Catalfamo D, Bradaschia-Correa V, Arana-Chavez V, Caridad AR, Neubert JK, Wronski TJ, Wallet SM, Holliday LS. 2012. Enoxacin directly inhibits osteoclastogenesis without inducing apoptosis. J Biol Chem 287:17894–17904. https://doi.org/10.1074/jbc.M111.280511.
26. Rivera MF, Chukkapalli SS, Velsko IM, Lee JY, Bhattacharyya I, Dolce C, Toro EJ, Holliday LS, Kesavalu L. 2014. Bis-enoxacin blocks rat alveolar bone resorption from experimental periodontitis. PLoS One 9:e92119. https://doi.org/10.1371/journal.pone.0092119.
27. Toro EJ, Zuo J, Guiterrez A, La Rosa RL, Gawron AJ, Bradaschia-Correa V, Arana-Chavez V, Dolce C, Rivera MF, Kesavalu L, Bhattacharyya I, Neubert JK, Holliday LS. 2013. Bis-enoxacin inhibits bone resorption and orthodontic tooth movement. J Dent Res 92:925–931. https://doi.org/10.1177/0022034513501876.
28. Campoccia D, Montanaro L, Arciola CR. 2006. The significance of infection related to orthopedic devices and issues of antibiotic resistance. Biomaterials 27:2331–2339. https://doi.org/10.1016/j.biomaterials.2005.11.044.
29. Riool M, de Boer L, Jaspers V, van der Loos CM, van Wamel WJB, Wu G, Kwakman PHS, Zaat SAJ. 2014. Staphylococcus epidermidis originating from titanium implants infects surrounding tissue and immune cells. Acta Biomater 10:5202–5212. https://doi.org/10.1016/j.actbio.2014.08.012.
30. Goodman SB, Yao ZY, Keeney M, Yang F. 2013. The future of biologic coatings for orthopaedic implants. Biomaterials 34:3174–3183. https://doi.org/10.1016/j.biomaterials.2013.01.074.
31. Pichavant L, Carrie H, Nguyen MN, Plawinski L, Durrieu MC, Heroguez V. 2016. Vancomycin functionalized nanoparticles for bactericidal biomaterial surfaces. Biomacromolecules 17:1339–1346. https://doi.org/10.1021/acs.biomac.5b01727.
32. Godoy-Gallardo M, Mas-Moruno C, Fernández-Calderón MC, Pérez-Giraldo C, Manero JM, Albericio F, Gil FJ, Rodríguez D. 2014. Covalent immobilization of hLf1-11 peptide on a titanium surface reduces bacterial adhesion and biofilm formation. Acta Biomater 10:3522–3534. https://doi.org/10.1016/j.actbio.2014.03.026.
33. Rodríguez-Cano A, Cintas P, Fernández-Calderón M-C, Pacha-Olivenza M-Á, Crespo L, Saldaña L, Vilaboa N, González-Martín M-L, Babiano R. 2013. Controlled silanization-amination reactions on the Ti6Al4V surface for biomedical applications. Colloids Surf B Biointerfaces 106:248–257. https://doi.org/10.1016/j.colsurfb.2013.01.034.
34. Scholar E. 2007. Enoxacin, p 1–6. xPharm: the comprehensive pharmacology reference. Elsevier, New York, NY.
35. Khoo X, O'Toole GA, Nair SA, Snyder BD, Kenan DJ, Grinstaff MW. 2010. Staphylococcus aureus resistance on titanium coated with multivalent PEGylated-peptides. Biomaterials 31:9285–9292. https://doi.org/10.1016/j.biomaterials.2010.08.031.
36. Pei J, Hall H, Spencer ND. 2011. The role of plasma proteins in cell adhesion to PEG surface-density-gradient-modified titanium oxide. Biomaterials 32:8968–8978. https://doi.org/10.1016/j.biomaterials.2011.08.034.
37. Branch DW, Wheeler BC, Brewer GJ, Leckband DE. 2001. Long-term stability of grafted polyethylene glycol surfaces for use with microstamped substrates in neuronal cell culture. Biomaterials 22:1035–1047. https://doi.org/10.1016/S0142-9612(00)00343-4.
38. Scott EA, Nichols MD, Cordova LH, George BJ, Jun Y-S, Elbert DL. 2008. Protein adsorption and cell adhesion on nanoscale bioactive coatings formed from poly(ethylene glycol) and albumin microgels. Biomaterials 29:4481–4493. https://doi.org/10.1016/j.biomaterials.2008.08.003.
39. Vermette P, Meagher L. 2003. Interactions of phospholipid- and poly(ethylene glycol)-modified surfaces with biological systems: relation to physico-chemical properties and mechanisms. Colloids Surf B Biointerfaces 28:153–198. https://doi.org/10.1016/S0927-7765(02)00160-1.
40. Ao H, Xie Y, Qin A, Ji H, Yang S, Huang L, Zheng X, Tang T. 2014. Immobilization of hyaluronic acid on plasma-sprayed porous titanium coatings for improving biological properties. J Biomater Sci Polymer Ed 25:1211–1224. https://doi.org/10.1080/09205063.2014.926577.
41. Palchesko RN, Buckholtz GA, Romeo JD, Gawalt ES. 2014. Co-immobilization of active antibiotics and cell adhesion peptides on calcium based biomaterials. Mater Sci Eng C 40:398–406. https://doi.org/10.1016/j.msec.2014.04.017.
42. Nie B, Ao H, Zhou J, Tang T, Yue B. 2016. Biofunctionalization of titanium with bacitracin immobilization shows potential for anti-bacteria, osteogenesis and reduction of macrophage inflammation. Colloids Surf B Biointerfaces 145:728–739. https://doi.org/10.1016/j.colsurfb.2016.05.089.
43. Tan HL, Ao HY, Ma R, Lin WT, Tang TT. 2014. In vivo effect of quaternized chitosan-loaded polymethylmethacrylate bone cement on methicillin-resistant Staphylococcus epidermidis infection of the tibial metaphysis in a rabbit model. Antimicrob Agents Chemother 58:6016–6023. https://doi.org/10.1128/AAC.03489-14.